

Evidence for grain growth in T Tauri disks[★]

F. Przygoda¹, R. van Boekel², P. Åbrahm³, S. Y. Melnikov⁴, L. B. F. M. Waters^{2,5}, and Ch. Leinert¹

¹ Max-Planck-Institut für Astronomie, Königstuhl 17, 69117 Heidelberg, Germany, email: przygoda@mpia.de

² Astronomical Institute “Anton Pannekoek”, University of Amsterdam, Kruislaan 403, 1098 SJ Amsterdam, The Netherlands

³ Konkoly Observatory of the Hungarian Academy of Sciences, H-1525 Budapest, P.O. Box 67, Hungary

⁴ Ulugh Beg Astronomical Institute, Academy of Sciences of Uzbekistan, Astronomical str. 33, Tashkent 700051, Uzbekistan

⁵ Instituut voor Sterrenkunde, Katholieke Universiteit Leuven, Celestijnenlaan 200B, B-3001 Heverlee, Belgium

Received 10 September 2003 / Accepted 6 November 2003

Abstract. In this article we present the results from mid-infrared spectroscopy of a sample of 14 T Tauri stars with silicate emission. The qualitative analysis of the spectra reveals a correlation between the strength of the silicate feature and its shape similar to the one which was found recently for the more massive Herbig Ae/Be stars by van Boekel et al. (2003). The comparison with theoretical spectra of amorphous olivine ($[\text{Mg},\text{Fe}]_2\text{SiO}_4$) with different grain sizes suggests that this correlation is indicating grain growth in the disks of T Tauri stars. Similar mechanisms of grain processing appear to be effective in both groups of young stars.

Key words. Stars: pre-main sequence – Stars: planetary systems: protoplanetary disks – Stars: circumstellar matter

1. Introduction

T Tauri stars are low mass young stellar objects with ages of 10^6 – 10^7 yr. One of the characteristics of so-called classical T Tauri stars is a distinctive IR excess. The origin of the IR radiation is the accretion disk which plays a crucial role in star formation by transporting material to the central star while angular momentum is transferred outwards. Different models were proposed to bring the observed facts into a general framework (Lynden-Bell & Pringle 1974; Adams, Lada, & Shu 1987; Chiang & Goldreich 1997). Yet there remain many open questions concerning the details of configuration, chemistry and evolution of disks. A particular feature of the infrared spectra of such disks is the silicate band in the region from 8 to $12\mu\text{m}$. The band originates from the stretching mode of the Si-O bond of silicate minerals like olivine ($[\text{Mg},\text{Fe}]_2\text{SiO}_4$), forsterite (Mg_2SiO_4), enstatite (MgSiO_3) and silica (SiO_2). The silicate feature observed in T Tauri stars appears in emission as well as in absorption (Cohen & Witteborn 1985). Silicate emission is assumed to emerge from a warm, optically thin disk layer (disk atmosphere) which is heated by the radiation of the central star (Chiang & Goldreich 1997, Natta, Meyer, & Beckwith 2000). Honda et al. (2003) showed that crystalline silicates are present in T Tauri stars, indicating substantial grain processing. In this Paper we present studies on the silicate emission from a sam-

ple of 14 T Tauri stars based on mid-infrared spectroscopy performed during three observation campaigns in February, June and December 2002 on the ESO 3.6 m telescope at La Silla. We analyse the spectra in particular with respect to a possible correlation between shape and strength of the silicate feature. Such a correlation has been recently observed for Herbig Ae/Be stars (van Boekel et al. 2003) and has been interpreted as evidence of grain processing in the circumstellar disks of those stars.

2. Observations and data reduction

The observations of the T Tauri stars were performed with TIMMI2, the Thermal Infrared Multi Mode Instrument 2 (Reimann et al. 1998) installed at the 3.6 m telescope at ESO’s observatory at La Silla, Chile. We observed each object in two modes: first we used the imaging mode to obtain photometry at $11.9\mu\text{m}$ (band width $1.2\mu\text{m}$). In a number of cases in addition we used the $8.9\mu\text{m}$ filter (band width $0.8\mu\text{m}$). Second we performed spectroscopy using the low-resolution grism mode ($R=160$) with a slit width of $1.2''$. In both modes the system was working with chopping and nodding with an amplitude of $10''$. In our data reduction, the measurements of the spectrophotometric standards were used to determine the shape of the spectra, and the photometric data at $11.9\mu\text{m}$ were used to establish the absolute flux level. The spectrum of the atmospheric extinction, which is needed to perform the first of these steps, was determined from observations of standard stars at different airmass. We regularly observed standard stars to monitor variations in atmospheric transmission. The flux data

Send offprint requests to: F. Przygoda

[★] Based on observations made with the ESO 3.6m Telescope at the La Silla Observatory under program ID 68.D-0537(A), 69.C-0268 and 70.C-0544.

Table 1. List of observed sources with the silicate feature in emission.

Object	Flux at 11.9 μm (Jy)	Observed at Run ^a	Multiple Source ^b	ISOPHOT spectrum available
AK Sco	2.1	B	*	*
AS 205	8.4	B	*	
CR Cha	0.8	C		*
DR Tau	2.0	C		*
GG Tau	0.8	C	*	
GW Ori	6.3	C	*	
Glass I	8.8	A,B,C	*	*
Haro 1-16	0.9	B		
HBC 639	2.3	A		
RU Lup	2.4	B		
S CrA	5.1	B	*	*
SU Aur	3.6	C	*	
TW Hya	0.6	C		
WW Cha	5.3	B,C		*

^a A: 5.+6. Feb. 2002, B: 7.+8. Jun. 2002, C: 24.-27. Dec. 2002

^b for AS 205 and S CrA we were able to obtain separate spectra of the components

for the spectrophotometric standard stars, (based on models by Cohen 1998), were taken from ESO's TIMMI2 webpage.

In total we observed 21 T Tauri stars with the silicate feature in emission. We selected the 14 objects for which the silicate feature was measured with a signal-to-noise ratio better than 2 (see Tab. 1). Several of these are known to be binary or multiple systems. In two cases we were able to obtain separate spectra of the components. The remaining 7 sources (DO Tau, DQ Tau, FU Ori, BBW 76, VZ Cha, VW Cha, Sz 82) were degraded by noise to the extent that a meaningful spectral analysis was not possible. For some stars the observations were repeated to verify the results.

For our studies we assumed that the continuum outside of the silicate band is actually reached at the edges of our measured spectral range (at 8.2 μm and at 13.0 μm). This assumption is supported by comparison of our spectra with ISOPHOT spectra (Ábrahám et. al 2003 in prep, see also Natta, Meyer, & Beckwith 2000). Figure 1 illustrates this for two examples. Here, the continuum was estimated by fitting a second order polynomial to all data points shortwards of 8 μm and beyond 12.8 μm . Note that the fitted curve is matching the ends of the TIMMI2 spectra and has an almost linear characteristic over the range of the silicate feature. Since we were not able to find such additional data of good quality for all objects of our sample, we estimated the continuum level within the silicate feature by a linear interpolation between the end points of the TIMMI2 spectra at 8.2 μm and at 13.0 μm , where the values for these end points were obtained by averaging over the data over an interval of 0.2 μm . The continuum level determined this way agreed with the second order fit, where available, to typically $\pm 10\%$. For all sources we consistently used the derived

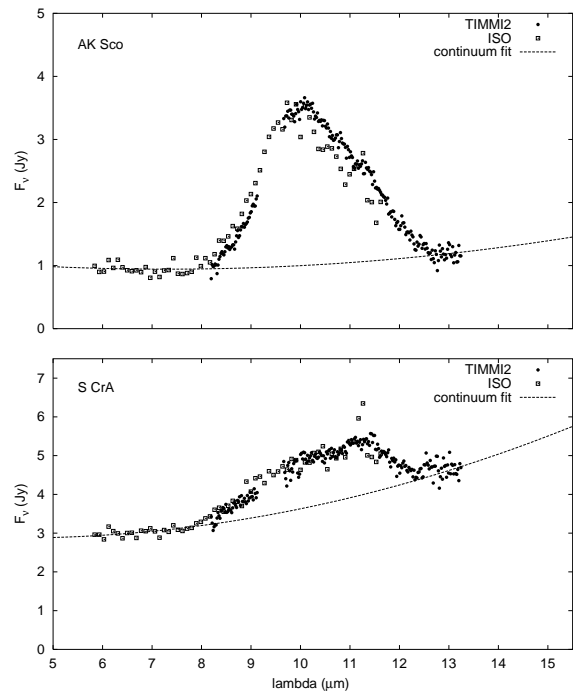


Fig. 1. Comparison of TIMMI2 and ISOPHOT data for two objects. The combined data were used to estimate the continuum by fitting a second order polynomial to the data points left of 8 μm and longwards of 12.8 μm .

linearly varying continuum level to determine the continuum normalized¹ spectra; these are shown in Fig. 2.

3. Analysis of the silicate feature

The spectra in Fig. 2 show a variety in strength and shape. In some spectra (AK Sco, Haro 1-16, CR Cha) a strong silicate emission with a peak near 9.8 μm is visible. In other cases (Ru Lup, DR Tau, HBC 639), the silicate emission is weaker and the profile looks more like a plateau. It is known that the shape of the band is strongly affected by the chemical composition and in particular by the size of the dust grains (Henning et al. 1995, Bouwman et al. 2001). A correlation between strength and shape of the silicate emission could be expected if there are systematic changes in particle size within the group of objects.

To estimate the strength of the silicate emission, we use the peak of the continuum normalised spectrum. For the characterisation of the band shape we measured the continuum subtracted flux at two wavelengths, 11.3 and 9.8 μm . The flux ratio for these wavelengths can be interpreted as a indicator for the grain size composition following Bouwman et al. (2001). They point out that (see Fig. 3)

- the mid-infrared absorption coefficient of small amorphous olivine dust grains (with a size of 0.1 μm) has a triangular shape with the maximum at 9.8 μm . This

¹ to preserve the shape of the emission feature we define:

$$F_{\text{norm}}(\lambda) = 1 + [F_{\text{total}}(\lambda) - F_{\text{continuum}}(\lambda)]/\langle F_{\text{continuum}} \rangle$$

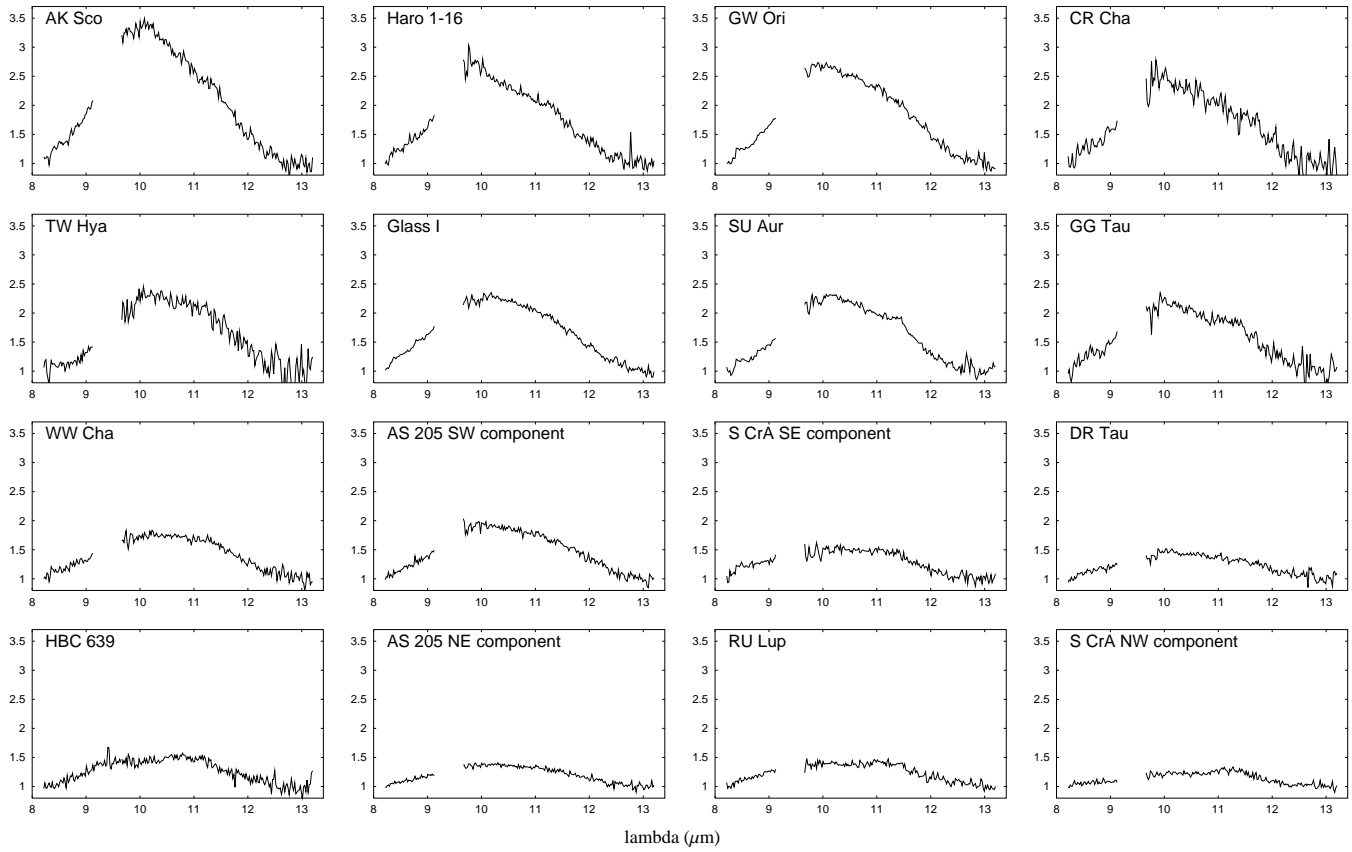


Fig. 2. Continuum normalized spectra of our sample ordered by the strength of the silicate feature. The shape of the feature is showing a correlation with the strength. Stronger features have a triangular shape with a pronounced peak near $9.8\,\mu\text{m}$ while weaker features are more plateau-like. The gap from 9.15 to $9.65\,\mu\text{m}$ in most of the spectra is caused by a broken channel of the TIMMI2 detector.

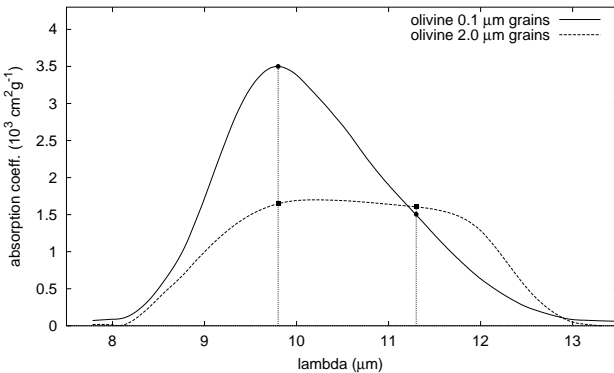


Fig. 3. Theoretical spectra of olivine dust with grain sizes of $0.1\,\mu\text{m}$ and $2.0\,\mu\text{m}$ (from Bouwman et al. 2001). The points at $9.8\,\mu\text{m}$ and $11.3\,\mu\text{m}$ are visualizing the dependence of the flux ratio at these wavelengths on the grain size.

Assuming a dust temperature of around 300 K, the blackbody thermal emission will not vary very much over our wavelength band, and the silicate emission profiles would have a shape quite close to the shape of the absorption coefficients. Since the absorption cross section per unit mass of large grains is in general smaller than that of small grains of similar shape, the emission of large grains is in general expected to be weaker than that of small grains.

Our observations suggest that most observed mid-infrared spectra of young low or intermediate mass stars can be characterised simply by emission corresponding to the two grain sizes covered in Fig. 4. We note that the ratio of absorption coefficients at the wavelengths of $11.3\,\mu\text{m}$ and $9.8\,\mu\text{m}$ as function of grain size varies from 0.43 (for $0.1\,\mu\text{m}$ grains) to about 1.0 ($2.0\,\mu\text{m}$ grains). Therefore, the ratio of the (continuum subtracted) flux at $11.3\,\mu\text{m}$ over that at $9.8\,\mu\text{m}$ should be a measure of the grain size. In Fig. 4 we plotted this ratio against the strength of the silicate feature. The distribution of the data points shows a clear correlation. Strong silicate features have $11.3/9.8$ flux ratios down to 0.53 (for CR Cha), while weak features exhibit higher ratios up to about 1.0 (in case of the S CrA NW-component even 1.42). The remaining points are distributed over the range between these two extremes. The error bars quoted in Fig. 4 take into account the signal to noise of the observations, and the uncertainty in the continuum estimate. A

spectrum is compatible with observations of the silicate emission of unprocessed dust of the ISM (see also Bowey, Adamson, & Whittet 1998).

- the mid-infrared absorption coefficient of larger amorphous olivine dust grains shows a plateau-like shape in the range from 9.5 to $12\,\mu\text{m}$.

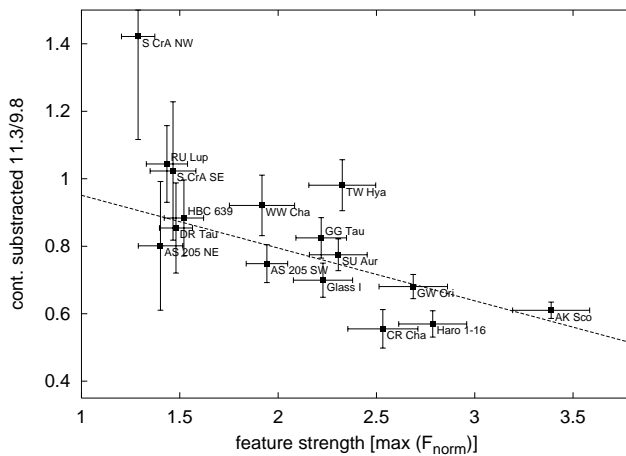


Fig. 4. Correlation between the strength of the silicate feature and the ratio of the (continuum subtracted) fluxes at $11.3\mu\text{m}$ over that at $9.8\mu\text{m}$. The strength is defined by the maximum of the silicate feature over the continuum.

weighted linear fit to the data points with the relation $y = a - bx$, where x is the strength of the feature and y the flux ratio, gives the coefficients: $a = 1.11 \pm 0.11$ and $b = -0.16 \pm 0.04$. A very similar correlation between strength and shape of the silicate emission was found by van Boekel et al. 2003 for isolated Herbig Ae/Be stars, with coefficients of $a = 1.48 \pm 0.09$, $b = -0.28 \pm 0.04$.

Emission by Polycyclic Aromatic Hydrocarbons (PAHs) at $11.3\mu\text{m}$ does not appear to be a problem for our data set. There was no evidence for PAH emission in our observed spectra nor in the available ISOPHOT-S spectra. This absence of PAH emission is not unexpected, since one can assume that the UV radiation of T Tauri stars normally is too weak to cause a significant excitation of PAH (Natta & Kruegel 1995).

4. Discussion

The large difference in geometric cross section per unit mass between large and small dust grains implies that if the silicate emission band is dominated by small grains, a substantial amount of large grains could be present without being noticed. On the other hand, the spectra with plateau-like emission are in general weak, likely due to a much lower number of small grains present in the upper disk regions. In some spectra (S CrA both components, RU Lup) the flux at $11.3\mu\text{m}$ is even higher than the flux at $9.8\mu\text{m}$, which results to a ratio greater than 1. This cannot be explained by the assumption of amorphous olivine dust with the absorption spectra shown above. It may be that crystalline forsterite (Mg_2SiO_4) is responsible for this effect, since its absorption spectrum shows a peak at $11.3\mu\text{m}$ (see Bouwman et al. 2001, Honda et al. 2003). Possible indications for crystalline forsterite are also seen in some other objects with stronger features (SU Aur, GG Tau).

We also note that the silicate emission emerges from warm, optically thin material, assumed here to be located in the upper layer of a flared accretion disk, which is irradiated by the central star. The dust in these upper layers of different T Tauri

disks appears to vary continuously between two extreme types: a) small amorphous dust grains or a mixture of small and large grains, with a spectrum very similar to the dust of the ISM and b) large amorphous dust grains with a possible addition of crystalline silicate. If we think of these differences in terms of evolution, then the reason for the difference between these two dust types could be either the removal of the small grains from the upper disk layers or the coagulation of small grains to larger ones. A removal of small dust grains by pure settling to the mid-plane of the disk is unlikely to explain the observed kind of differentiation since the settling time for larger grains is shorter than for the smaller ones. A further mechanism which could be responsible for the vanishing of small grains is by the radiation pressure of the central star. A star of solar luminosity would be quite effective in removing tenth micron sized particles. But in this case, a permanent diffusion of particles from the mid-plane on shorter time scales should avoid a significant decrease of the amount of small particles in the upper layer (Takeuchi & Lin 2003). The effect of coagulation is a possible explanation, if constructive collisions to larger grains dominate over destructive collisions which produce again small grains. This should be the case in T Tauri disks where the SED can be well fit by gas-rich disks in hydrostatic equilibrium.

An interesting detail of our studies is the availability of separate spectra from the components of two binary T Tauri systems (AS 205 and S CrA). We observed significant differences in strength and also differences in the shape of the silicate band of the components, with the secondary having the - relatively - stronger emission. Since the components presumably have the same age, the difference must have other reasons than the evolutionary state of the stars.

Acknowledgements. This work is partly supported by the Hungarian Research Fund (OTKA No. T037508) and by the Bolyai Fellowship (P. Ábrahám). S. Y. Melnikov thanks the German Academic Exchange Service (DAAD) for the DAAD fellowship grant.

References

- Adams, F. C., Lada, C. J., & Shu, F. H. 1987, ApJ, 312, 788
- van den Ancker, M. E., Wesselius, P. R., Tielens, A. G. G. M., van Dishoeck, E. F., & Spinoglio, L. 1999, A&A, 348, 877
- van Boekel, R., Waters, L. B. F. M., Dominik, C., Bouwman, J., de Koter, A., Dullemond, C. P., & Paresce, F. 2003, A&A, 400, L21
- Bouwman, J., Meeus, G., de Koter, A., Hony, S., Dominik, C., & Waters, L. B. F. M. 2001, A&A, 375, 950
- Bowey, J. E., Adamson, A. J., & Whittet, D. C. B. 1998, MNRAS, 298, 131
- Chiang, E. I. & Goldreich, P. 1997, ApJ, 490, 368
- Cohen, M. & Witteborn, F. C. 1985, ApJ, 294, 345
- Cohen, M. 1998, AJ, 115, 2092
- Henning, T., Begemann, B., Mutschke, H., & Dorschner, J. 1995, A&AS, 112, 143
- Honda, M., Kataza, H., Okamoto, Y. K., Miyata, T., Yamashita, T., Sako, S., Takubo, S., & Onaka, T. 2003, ApJ, 585, L59
- Lynden-Bell, D. & Pringle, J. E. 1974, MNRAS, 168, 603
- Natta, A. & Kruegel, E. 1995, A&A, 302, 849
- Natta, A., Meyer, M. R., & Beckwith, S. V. W. 2000, ApJ, 534, 838
- Reimann, H., Weinert, U., & Wagner, S. 1998, Proc. SPIE, 3354, 865
- Takeuchi, T. & Lin, D. N. C. 2003, ApJ, 593, 524